



Article

Application of Electrical Resistivity Tomography in Geotechnical and Geoenvironmental Engineering Aspect

Md Jobair Bin Alam ^{1,*}, Asif Ahmed ² and Md Zahangir Alam ³

¹ Department of Civil and Environmental Engineering, College of Engineering, Prairie View A&M University, Prairie View, TX 77446, USA

² College of Engineering, SUNY Polytechnic Institute, Utica, NY 13502, USA; asif.ahmed@sunypoly.edu

³ Planning/Engineering Studies, California Department of Transportation, San Bernardino, CA 92401, USA; md.z.alam@dot.ca.gov

* Correspondence: mdalam@pvamu.edu

Abstract: Electrical resistivity tomography (ERT) has turned out to be one of the most applied and user-friendly geophysical methods in geotechnical and geoenvironmental research. ERT is an emerging technology that is becoming popular nowadays for investigating subsurface conditions. Multiple attributes of the technology using various electrode configurations significantly reduce measurement time and are suitable for applications even in hardly accessible mountain areas. It is a noninvasive test for subsurface characterization and a very sensitive method used to determine geophysical properties, i.e., structural integrity, water content, fluid composition, etc. This paper aimed to elucidate the ERT technique's main features and applications in geotechnical and geoenvironmental engineering through four case studies. The first case study investigated the possible flow paths and areas of moisture accumulation after leachate recirculation in a bioreactor landfill. The second case study attempted to determine the moisture variation along highway pavement. The third case study explored the slope failure investigation by ERT. The fourth case study demonstrated the efficiency of the ERT method in the landfill evapotranspiration (ET) cover to investigate moisture variation on a broader scale and performance monitoring. In all of the four cases, ERT exhibited promising performance.



Citation: Alam, M.J.B.; Ahmed, A.; Alam, M.Z. Application of Electrical Resistivity Tomography in Geotechnical and Geoenvironmental Engineering Aspect. *Geotechnics* **2024**, *4*, 399–414. <https://doi.org/10.3390/geotechnics4020022>

Academic Editor: Mahdi M. Disfani

Received: 16 January 2024

Revised: 26 March 2024

Accepted: 2 April 2024

Published: 4 April 2024



Copyright: © 2024 by the authors. Licensee MDPI, Basel, Switzerland. This article is an open access article distributed under the terms and conditions of the Creative Commons Attribution (CC BY) license (<https://creativecommons.org/licenses/by/4.0/>).

Keywords: electrical resistivity tomography; pavement; slope failure; ET cover; seasonal variation; landfill; leachate circulation

1. Introduction

Electrical resistivity tomography is a subsurface profiling technique that records hundreds of subsurface data points which are used to produce a monochrome or multicolored two-dimensional cross-section of the earth. In recent years, electrical resistivity surveys have progressed rapidly from the conventional sounding survey. This technique is capable of measuring both horizontal and vertical variability of soil arrangement over several meters of the perspective area [1]. It is a nondestructive test, and the purpose of electrical surveys is to determine the subsurface resistivity distribution by making measurements on the ground surface and also characterize subsurface properties, i.e., structure, water content, or fluid composition [2]. This method is widely used in hydrogeological, environmental, and geotechnical research as it can potentially reveal the subsurface image [3–10]. This technique is used for the investigation of morphotectonic [11], weathering studies [12], landform evolution in mountain areas [13], permafrost detection [14], and exploration of underground karst structures [15]. With the progress of the ERT technique, 2D resistivity is more popular in investigating geophysical and geohazard conditions [16] as it has a simple method of data interpretation. The ERT method follows Ohm's law where the resulting potential differences are measured by transferring artificially generated currents

to the soil [2]. The electrical resistivity depends on several factors of the subsurface conditions. The subsurface soil moisture and temperature [17], degree of saturation [18], organic content [19], pore water composition [20], and geologic formation [21] are some of the factors. Where there is heterogeneity between the soil matrixes, the subsurface image from ERT comes out with different contrasts. Based on the requirements and purposes, one-, two-, three-, and four-dimensional ERT surveys are conducted [1,2,22]. Laboratory calibration is basically performed by a one-dimensional array while the two-dimensional arrays are used to depict the vertical subsurface image. Three-dimensional arrays are used where there is a wide range of anisotropy and soil variability, especially in waste disposal sites [23]. However, the 2D electrical tomography method gives appropriate results when the resistivity contrast is high. Additionally, ERT is widely used nowadays for determining the soil's intrinsic properties.

ERT is a sophisticated technology to explore subsurface conditions. It is becoming more popular with researchers of geotechnical and geoenvironmental fields as the data acquisition system in this method is user-friendly and provides large-scale data. In the last decades, software was developed by the Schlumberger brothers to convert the resistivity data into images to interpret the subsoil condition in terms of ohm-m unit [2]. The resistivity profile in the image form provides a broad interpretation of the subsurface conditions. The most encouraging and important part of it is that it gives a broader spectrum of the soil moisture distribution within the area of interest [24]. That is why the ERT technique is now often used in landfills to inspect the moisture variation in the landfilled waste and the rate of waste degradation to have controlled leachate generation [25]. Apart from this, ERT technology is now vastly being used in geotechnical investigation [4–10,21,26]. To determine the unknown foundation depth, slope failure investigation, crack detection, the existence of sinkholes, foundation failure, moisture variation in pavement base materials, soil movement, etc., are broadly examined by the ERT method. The results are very promising [24,27].

Estimation of the hydraulic parameters of the soil of earth infrastructures (e.g., slope, pavement subgrade, landfill cap, etc.) is typically executed through sensor technology such as capacitance sensors, thermal dissipation sensors, psychrometers, tensiometers, and time domain reflectometers (TDRs) [28]. These methods provide precise measurements of the hydraulic parameters at the installation points. However, the Earth infrastructure system can be moderate to massive in size where the point information may not be well representative. The longitudinal extent of an earthen embankment can be 300 to 400 feet or even more. Hence, sensors installed at certain locations in the embankments may not be exemplary. Similarly, the pavement section can be long enough to rely on the point information for effective investigation. However, the ERT methods provide a complete pictorial view of the subsurface. As such, perched water zones and moisture intrusion locations can be detected precisely through the ERT method. In addition, evaluating seasonal moisture variation through the ERT method provides a broader aspect of the soil behavior at various climatic conditions.

Landfills are massive in size, and monitoring of the landfilled waste properties is quite difficult and expensive using sensors. Moreover, the extreme heterogeneity of solid waste may pose a serious threat to the malfunctioning of sensors. For landfill covers, considering the size of landfills where several acres of the area would have been required to construct ET cover, point measurements of the significant hydraulic parameters may not be well representative for performance evaluation and decision making in design modifications. Sensors may be installed at multiple locations and at multiple depths in the entire cover area to produce ample monitoring data. However, sensor installation is expensive, and sensors may not last long on the ground. As a result, reinstallation may be required, which will bring about additional costs. Furthermore, sensor installation is destructive to the cover system. Accordingly, it damages the integrity of the cover and deteriorates the cover's performance. Therefore, an alternative nondestructive testing method to determine the moisture variation in the cover system and to quantify the hydraulic parameters is crucial.

ERT, being a nondestructive geophysical method, would potentially provide the solution of ET cover performance monitoring. The manuscript's authors were affiliated with the four case studies presented here. The authors were part of the field investigation, data collection, and analysis of the data.

2. Theory of ERT

2.1. Basic

ERT is a geophysical technique where, using two transmitting electrodes and a current injection, an electric potential field is created, and the resulting potential change is measured between the two receiving electrodes [29]. Electrical resistivity quantifies how strongly a material opposes the flow of an electric current. The spacing between the transmitting and receiving electrodes determines the spatial resolution and volume of interrogation over which each measurement is collected. The theory of ERT is applicable in an entirely homogeneous half-space medium. Soil resistivity value can be calculated for the subsurface by knowing the magnitude of the injected current and measuring the resulting electric potential at specific locations. However, subsurface homogeneity is very rare in natural conditions, and electric current, when injected, will follow the path of least resistance [30]. Figure 1 conceptualizes the subsurface electric current flow and the influence of subsurface heterogeneities.

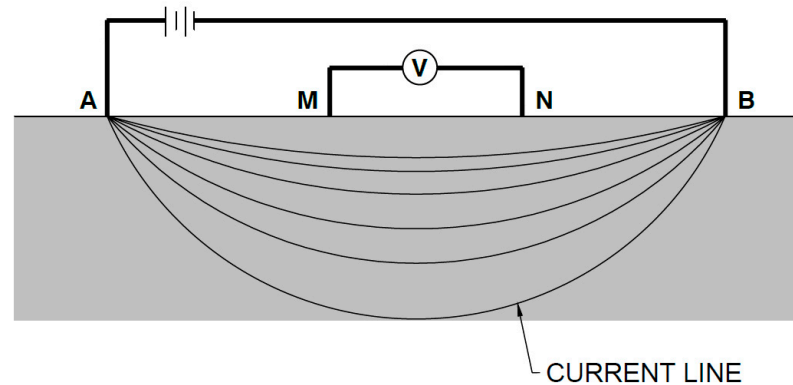


Figure 1. Variations in subsurface electric current density (redrawn from [3]). At least four electrodes are required for electrical resistivity measurement. A, B are the current electrodes (through which electricity passes) whereas M, N are the potential electrodes (through which potential differences are measured), and V is the voltage.

For a simple soil body, the resistivity ρ (ohm-m) is defined as follows [30] (Figure 2):

$$\rho = R (A/L)$$

where R is the electrical resistance, L is the cylinder length (m), and A is the cross-section area (m^2). Ohm's law defines the electrical resistance of a cylindrical body as defined by [31].

$$R = V/I,$$

where V is the potential difference measure in volt, and I is the current in ampere. The current density J (A/m^2) is determined according to [30] for all the radial directions, with

$$J = I/A = (I/ 2\pi r^2),$$

where $2\pi r^2$ is the surface of a hemispherical sphere of radius r. This formula considers the curved surface area of the hemisphere. The factor of 2 is included because a full sphere has a surface area of $4\pi r^2$, and a hemisphere is just half of that.

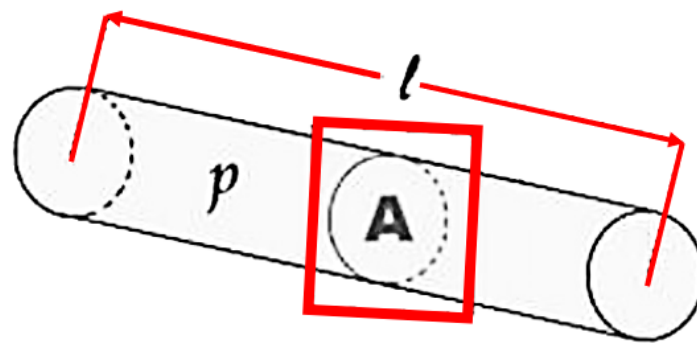


Figure 2. Relation between resistance and resistivity (redrawn from [1]).

Typically, four electrodes are necessary to compute the electrical resistivity of soil. Electrodes A and B are known as current electrodes, and M and N are known as potential electrodes (Figure 3). Current is passed through A and B and the potential difference is measured by M and N. The schematic of the process is shown in Figure 3.

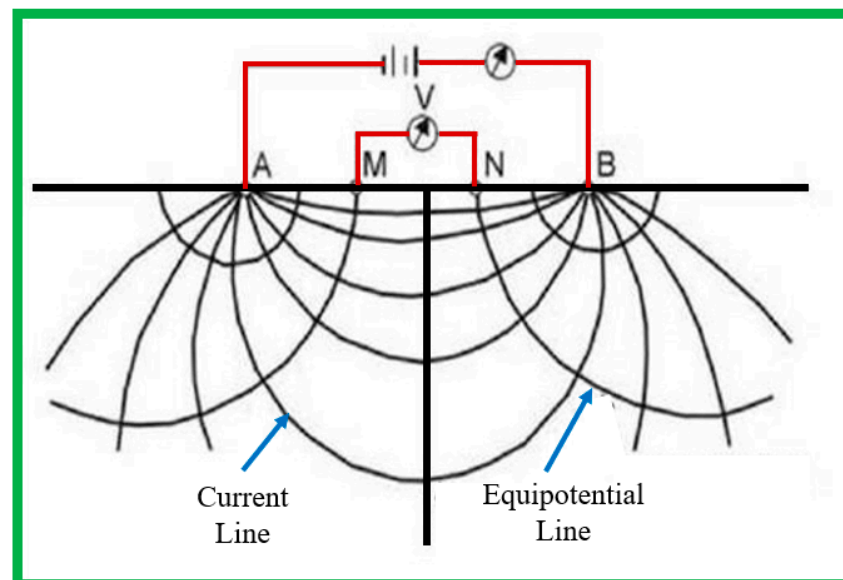


Figure 3. Equipotential and current lines for a pair of current electrodes (redrawn from [32]). A and B are the current electrodes, and M and N are the potential electrodes, and V is the voltage.

2.2. Data Acquisition

Different types of array configurations are available based on the respective positions of the potential electrodes and the current electrodes. The most commonly used array configurations are Wenner, Wenner–Schlumberger, dipole–dipole, pole–pole, and pole–dipole which are presented in Figure 4. Each ERT array type has its benefits and drawbacks, so it is common practice to test multiple ERT arrays at the beginning of a survey to determine which array has the best resolution for the desired survey requirements. In the current studies, field investigation was performed by utilizing a SuperSting R8/IP resistivity meter (Advanced Geosciences, INC., Austin, TX, USA) and a dipole–dipole array configuration. In the resistivity tomography method, the electrode spacing depends on several parameters, i.e., required resolution for site investigations, size of objects under investigation, and depth of penetration required for the site investigations. A better resolution may be achieved using smaller electrode spacing, whereas the penetration depth will be smaller. For the same number of electrodes, a larger penetration depth would come under larger electrode spacing. Therefore, a total of 56 electrodes with 6 feet spacing

were utilized in the landfill study, whereas a total of 28 electrodes with 3 feet spacing were utilized in the other two studies. A 12 V battery was utilized to perform the ERT in the field.

	Electrodes Array	K
2D Wenner	A \xleftrightarrow{a} M \xleftrightarrow{a} N \xleftrightarrow{a} B	$2\pi a$
Wenner-Schlumberger	A \xleftrightarrow{na} M \xleftrightarrow{a} N \xleftrightarrow{na} B	$\pi n(n+1)a$
Dipole-Dipole	A \xleftrightarrow{a} B \xleftrightarrow{na} M \xleftrightarrow{a} N	$\pi n(n+1)(n+2)a$
Pole-Pole	B \xleftrightarrow{a} A \xleftrightarrow{a} M \xleftrightarrow{a} N	$2\pi a$
Pole-Dipole Forward	A \xleftrightarrow{na} M \xleftrightarrow{a} N	$2\pi n(n+1)a$
Reversed	M \xleftrightarrow{na} N \xleftrightarrow{a} A	

Figure 4. Different array configuration for 2D resistivity tomography (redrawn from [2]). A,B are current electrodes; M, N are potential electrodes; ‘a’ is the distance between adjacent electrodes; ‘n’ is the ratio of the distance between the current and potential electrodes.

2.3. Data Interpretation

There are two methods in electrical resistivity data processing and interpretation, known as inversion and forward modeling. To perform one process, the other process must also be performed. An image is presented converting the field investigation data, and then the apparent resistivity is calculated based on the test injected current and resulting potential difference [33]. With the known array type and apparent resistivity, a profile named a pseudosection is created. The pseudosection provides the necessary data for inversion. Numerical analysis software like RES2DINV, RES3dINV, and EarthImager 1D, 2D, and 3D are operated to perform the inversion process (Figure 5).

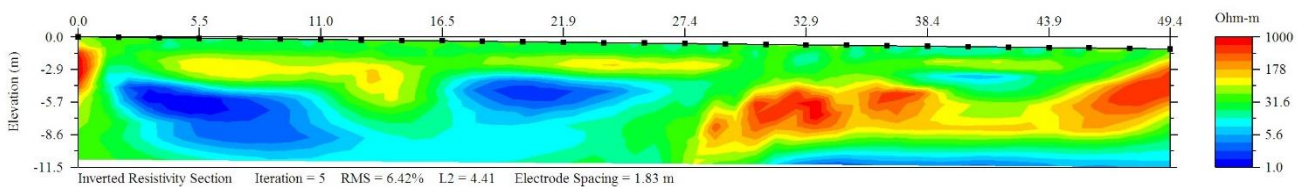


Figure 5. Data interpretation in EarthImager 2D software.

In the current studies, the apparent resistivity data were collected and stored as a raw format after finishing the ERT test. The raw data were downloaded from the SuperSting R8/IP meter ((Advanced Geosciences, INC., Austin, TX, USA) using AGI Administrator software and we converted field data to a readable format for the AGI EarthImager 2D analysis software (version 2.1). An inverted resistivity section was recreated from the measured apparent resistivity pseudosection by using the AGI EarthImager 2D software. Inversion is a subsurface resistivity distribution plotting process that uses measured apparent resistivity. EarthImager 2D software can perform forward modeling, damped least squares inversion, smooth model inversion, and robust inversion. In the current studies, a robust inversion model was utilized. In the inversion process, the number of iterations was 8, the error reduction was 3%, and the maximum RMS error was limited to 3%. The minimum resistivity value was selected to 1 ohm-m, while the maximum value was set to 50,000 ohm-m. The resolution factor was selected as 0.2, and the horizontal/vertical roughness ratio was selected as 1. Regarding the robust data conditioner, the authors used the default value of 10.

3. Case Studies

The four case studies included in this manuscript are moisture (leachate) flow distribution due to leachate recirculation in bioreactor landfill or enhanced leachate recirculation operation, pavement moisture variation, slope failure investigation, and moisture variation in water balance or evapotranspiration (ET) cover under varied climatic patterns. In the field studies, 28/56 electrodes were used in different projects at varied spacing based on the project requirements. The electrodes used in all the projects were 2 feet long.

3.1. Case Study 1: Determination of Leachate Recirculation Frequency in Denton Landfill

The objective of this study was to investigate the probable flow paths and zones of moisture accumulations after leachate recirculation in the specific cells of the landfill during the bioreactor operation. Two-dimensional resistivity tomography was accomplished to determine the moisture distribution in landfilled waste, which led to the path to evaluate the leachate recirculation frequency. The field setup during the field investigation at the site is shown in Figure 6.



Figure 6. The authors conducting resistivity tomography at the site.

3.1.1. Description

The City of Denton municipal solid waste (MSW) landfill started its operation in 1984. The landfill receives approximately 500 to 600 tons of waste per day based on the information gathered in 2009. The landfill received the regulatory permit to operate as an ELR (enhanced leachate recirculation)/bioreactor landfill in May 2009 [26,34]. In bioreactor landfills, regular moisture/leachate circulation is required for rapid decomposition of the waste. To decompose the waste effectively, the landfill operators need to know two crucial pieces of information: (i) the current moisture condition in the landfilled waste, and (ii) how frequently recirculation operation is required, and where to recirculate.

3.1.2. Result

The City of Denton landfill had installed multiple recirculation pipes for the bioreactor operation. In this study, three recirculation pipes (H2, H16, and H18) were selected for the years May 2010 to April 2013 to investigate moisture movement into the waste. Resistivity tests were conducted for each recirculation pipe one day, seven days, and fourteen days after leachate recirculation to understand the leachate/moisture flow characteristics. For simplicity, the resistivity tomography results of one pipe (pipe: H2) are only presented here, as other pipes showed similar patterns. The results of the field investigation around pipe H2 (in the vicinity of the dotted circle) are presented in Figure 7. The moisture content of the waste around the three pipes was determined using correlation [35], which is presented in Table 1. It is to be noted that the moisture contents of the waste were determined around

these pipes for the entire study. However, Table 1 presents the moisture contents estimated below the pipes only.

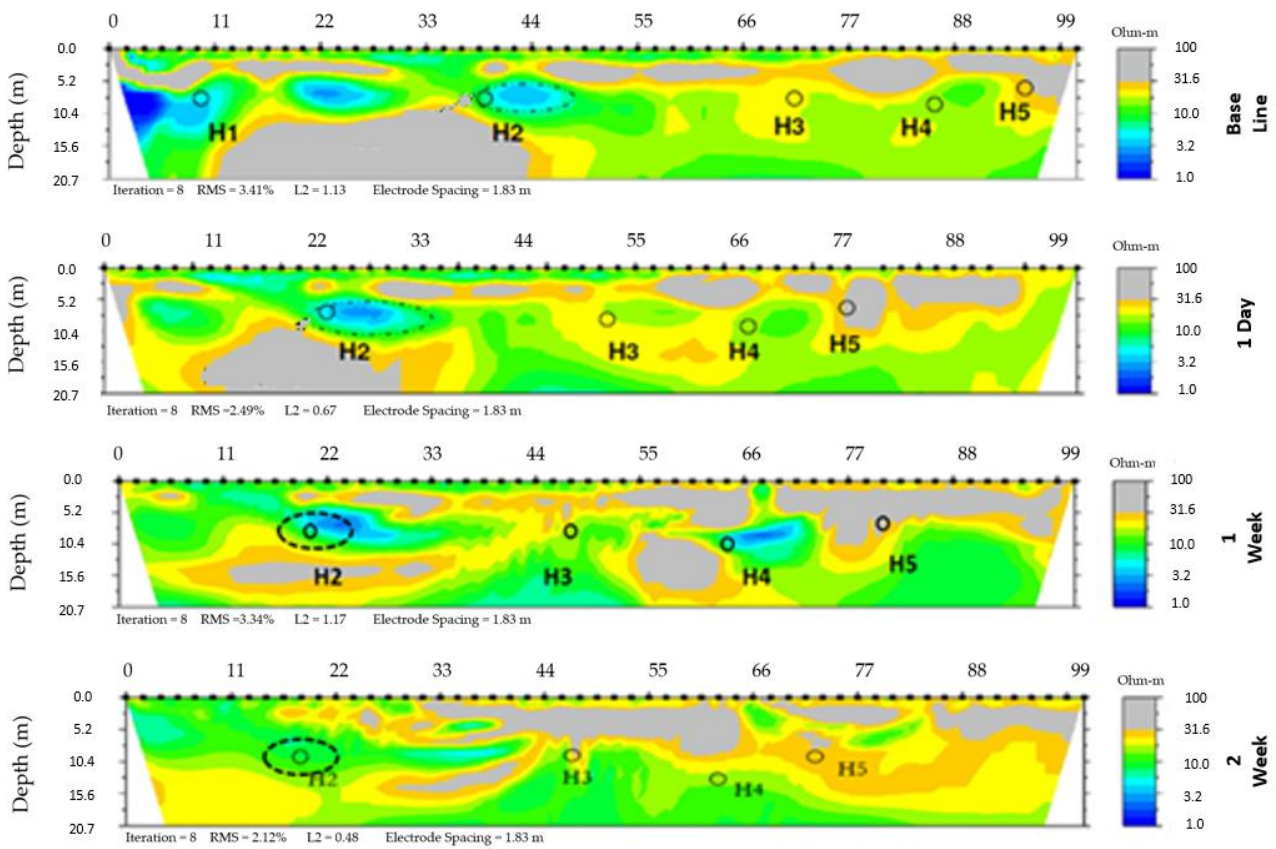


Figure 7. Resistivity tomography results of pipe H2.

Table 1. Moisture content of waste around pipes H2, H16, and H18.

	Base Line	1 Day	1 Week	2 Week
Pipe	MC (%)	MC (%)	MC (%)	MC (%)
H2	36.31	63.35	49.77	36.78
H16	31.48	59.38	47.03	32.68
H18	33.09	63.35	45.16	31.02

From Table 1, for recirculation pipe H2, the moisture content is 36.31% at the baseline condition, which represents the moisture condition of the waste at the existing condition just before the leachate recirculation. One day after leachate recirculation, moisture content increases significantly to 63.35% around pipe H2. It becomes 49.77% after 1 week and 36.78% after 2 weeks. The reduction in the moisture content in these two weeks signifies that leachate traveled into the waste after recirculation. This can be further comprehended by looking at the qualitative assessment of the resistivity profile. In the baseline (Figure 7), there is a grey area (high resistivity or low moisture content) below the recirculation pipe, which completely disappears just one day after the recirculation as that area turns green to moderate green or yellow (low resistivity or high moisture). It is also to be highlighted that the moisture content of the waste around the pipes at the baseline condition and 2 weeks after recirculation is very close in magnitude. This trend is similar to other recirculation pipes. As such, in each case, moisture content drops very close to baseline after fourteen days of leachate recirculation. As a result, it is reasonable to conclude that the frequency of leachate recirculation for bioreactor operation will be fourteen days (2 weeks) from the initial injection [27]. In this case, the ERT method provided a continuous portrayal of the

landfill waste of almost 18.2 m (60 feet). This broader evaluation of leachate recirculation and waste moisture content would not have been possible using sensor technology for effective ELR operation.

3.2. Case Study 2: Use of Resistivity Tomography in Pavement Moisture Distribution

Moisture movement beneath a pavement causes uneven deformation in the expansive pavement subgrade. Resistivity can provide valuable information regarding moisture movement beneath a pavement [36,37]. As such, a geophysical investigation was conducted using the ERT technique on the State Highway (SH) 342 located in Lancaster, Texas. Figure 8a shows the ERT field setup at the pavement slope, and the line (red) on which ERT was conducted is shown in Figure 8b.

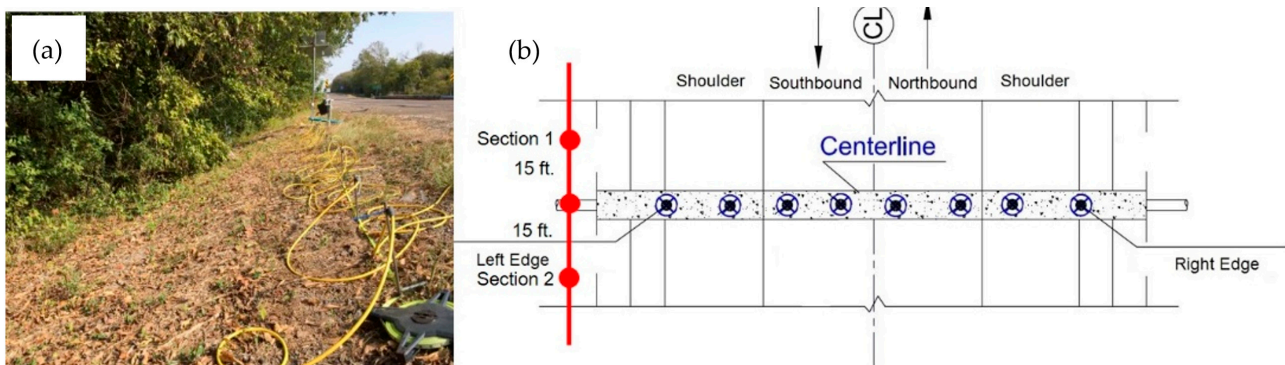


Figure 8. (a) ERT experiment on pavement slope; (b) schematic of the location.

3.2.1. Description

The objective of conducting the ERT test on the pavement side slope was to observe the seasonal distribution of soil moisture. The resistivity test was conducted every month. For convenience, only a few months' plots are shown in the manuscript. Resistivity tomography was conducted for two years from 2015 to 2017. Seasonal variation of the moisture in pavement helps to understand the deformation profile of the flexible pavement in Texas built on expansive soil [38].

3.2.2. Result

Two resistivity plots are shown in Figure 9. Figure 9a indicates the higher resistivity zone at the first few feet of the pavement slope. On the contrary, the resistivity values changed to lower values as shown in Figure 9b. It was found from field analysis that the May–October months' ERT plots were showing higher resistivity values, whereas November to April was exhibiting lower resistivity values. As such, May–October was identified as the dry period, and November–April was marked as the wet period for the pavement. Another interesting observation was noticed in Figure 9c from May 2016. It was observed that there is a low-resistivity zone at the center at around 3 feet, indicating the presence of moisture. Resistivity conducted this month was after rainfall events which shows the moisture intrusion into the pavement because of the existence of edge cracks. Field visits made during the study confirmed the presence of cracks.

A similar trend was observed in the 2016–2017 monitoring period (Figure 10). As with the previous year, November to April was found to be a wetter period, while May to October was found to be drier, confirming the seasonal moisture variation in the pavement.

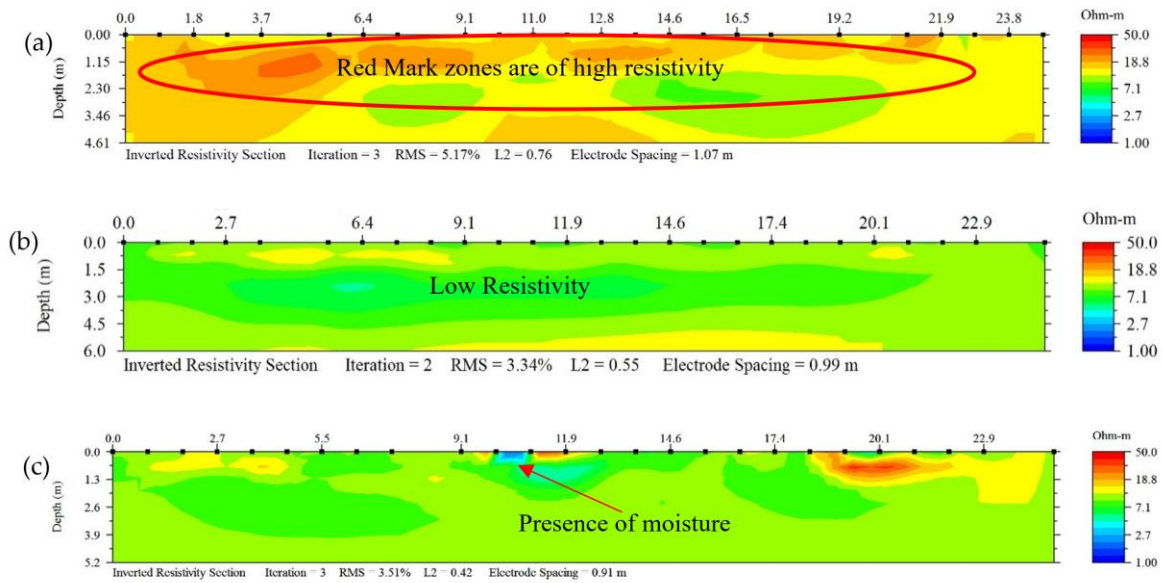


Figure 9. Monthly resistivity plots: (a) higher resistivity; (b) low resistivity; (c) moisture intrusion.

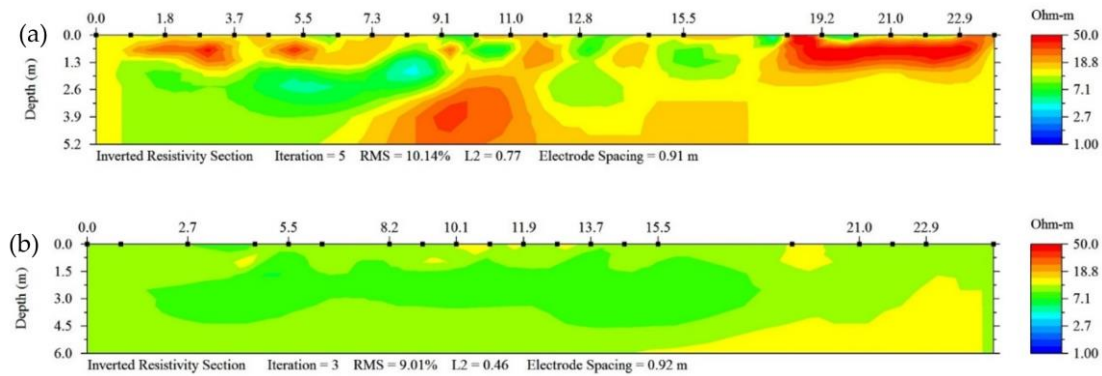


Figure 10. (a) Typical dry period (2016–17); (b) typical wet period (2016–17).

The following plots discuss the change in resistivity over different times of the year at different depths taken at two different sections (Figure 11). Two sections were taken 4.5 m (15 feet) apart at both sides from the center line, as shown in Figure 8. As observed, there was a seasonal trend in the resistivity values. Values at different depths posed a higher value in the dry period, whereas lower values in the wet period. The amplitude of variation decreased with depth. For example, the resistivity value at 1 m depth dropped from 22 ohm-m (October 2015) to 11 ohm-m (December 2015) in Section 1, which corresponded to a 50% drop in value (Figure 11a). It maintained a resistivity value of around 10 ohm-m from December 2015 to May 2016. Resistivity observed at 2 m depth decreased from 11 ohm-m (October 2015) to 8.5 ohm-m (April 2016), which corresponded to a 22% decrease in resistivity. Again, it increased to a value of 14 ohm-m in June 2016, which indicated the seasonal response. It is expected to have higher values in the next months of 2016 till October.

Similar observations were recorded in Section 2 (Figure 11b). Resistivity at 1 m depth experienced a 26.7% drop from October 2015 to May 2016. At 1.5 m, it experienced a 30% increase from April to June 2016 after a 27% drop from October 2015. Similarly, a 20% drop and a 27% increase were observed at 2 m depth. As can be seen, the greater variation was observed at the upper depth. The difference between drop and rise decreased with increased depth from the surface. A similar trend was observed in the following year, 2016–2017. In April 2016, 4.52 inches of rainfall were recorded, followed by 4.94 inches in May 2016. However, June 2016 saw only 2.63 inches, and July 2016 registered merely

1.63 inches. This downward trend in rainfall was mirrored in the resistivity value for July 2016. Thus, it can be inferred that variations in resistivity values are linked to both seasonal changes and rainfall, with seasonal factors playing a predominant role.

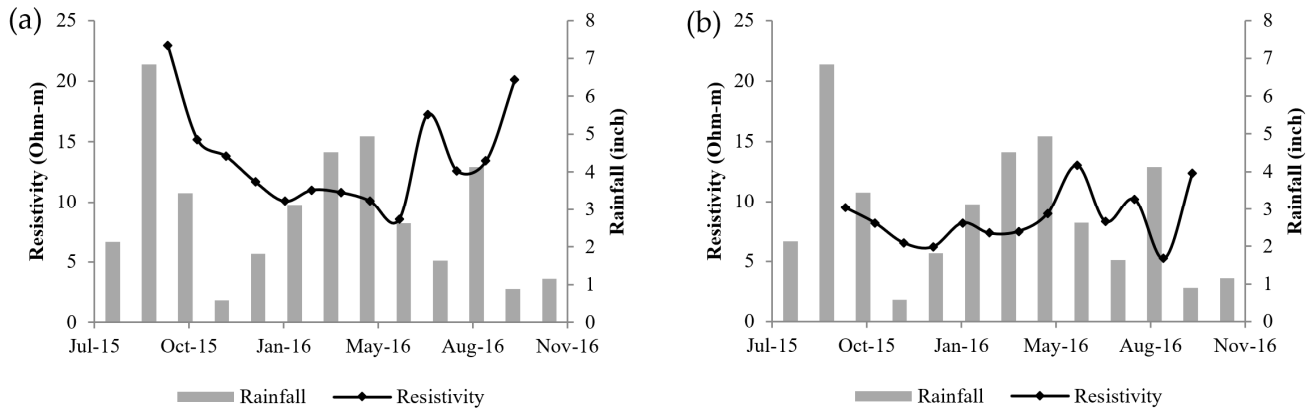


Figure 11. Change in resistivity with rainfall at (a) 0.91 m (2 feet) and (b) 3.05 m (10 feet).

3.3. Case Study 3: Resistivity Tomography in Slope Failure Investigation

Shallow slope failure in expansive soil is a widespread phenomenon in Texas. Due to the wetting–drying nature of the expansive clay because of varied climatic conditions, highway slopes often fail after the summer season followed by a heavy rainfall event [39]. The objective of this study was to analyze the failure of a highway slope using the ERT method.

3.3.1. Description

The study was conducted on the slope along the highway US 183. After the summer of 2013, there was a desiccation crack on the slope which created a path for possible intrusion of rainwater (Figure 12a). The presence of a high-moisture zone was observed within 2.1 m (7 feet) of the slope, which indicated a perched water zone because of the crack in the slope [40,41]. In September 2014, the slope failed (Figure 12b) due to the fully softened condition of the soil near the crack.



Figure 12. (a) Cracks on the shoulder; (b) failure at the crest of the slope.

3.3.2. Result

Figure 13a shows the failure condition of US 183 slope. There are two failure areas there, one at the top and another at the middle of the slope. There is a visible crack in the middle of the slope. Based on the resistivity tomography profile at resistivity line (RL)-1 (Line 1 in Figure 13b), a high-resistivity zone was observed up to the top 2.1 m (7 feet) depth (Figure 14a), which might indicate the existence of a low-moisture zone near the

top of the slope. It should be noted that the resistivity tomography test was conducted during the dry period. Therefore, it can reasonably be inferred that the low-moisture zone indicates the active zone or zone of seasonal moisture variation. Moreover, a low-resistivity zone was present in RL-1 after 2.1 m (7 feet) depth, which might indicate the presence of high moisture below the active zone.

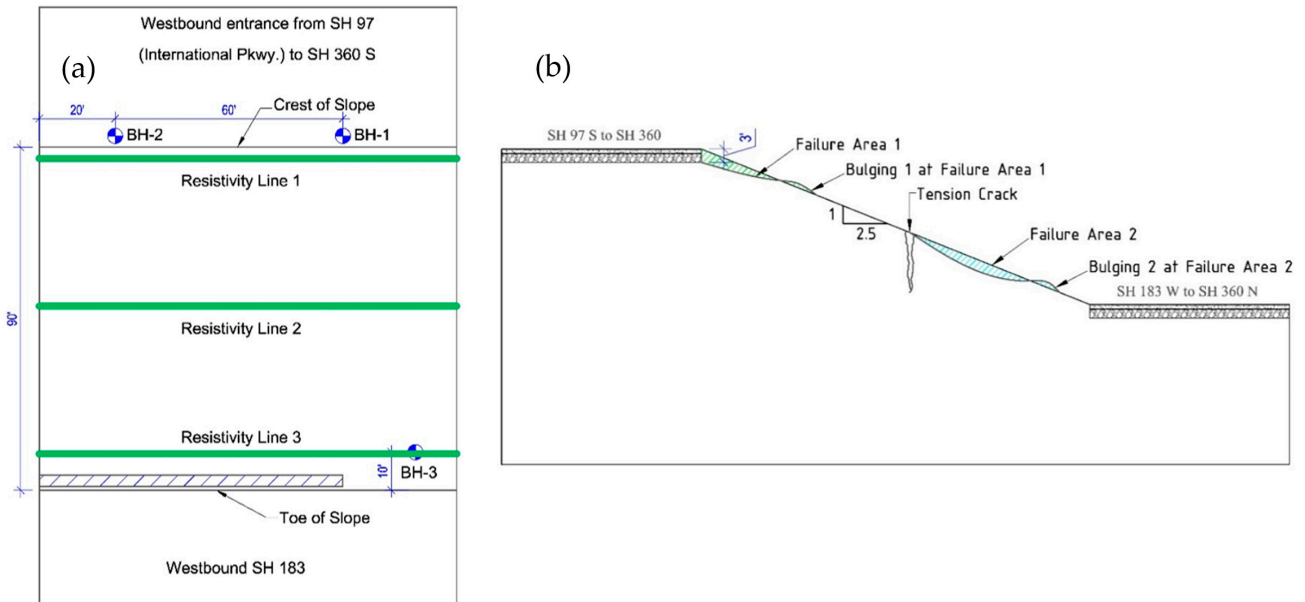


Figure 13. (a) Failure condition of SH 183; (b) resistivity lines along the slope.

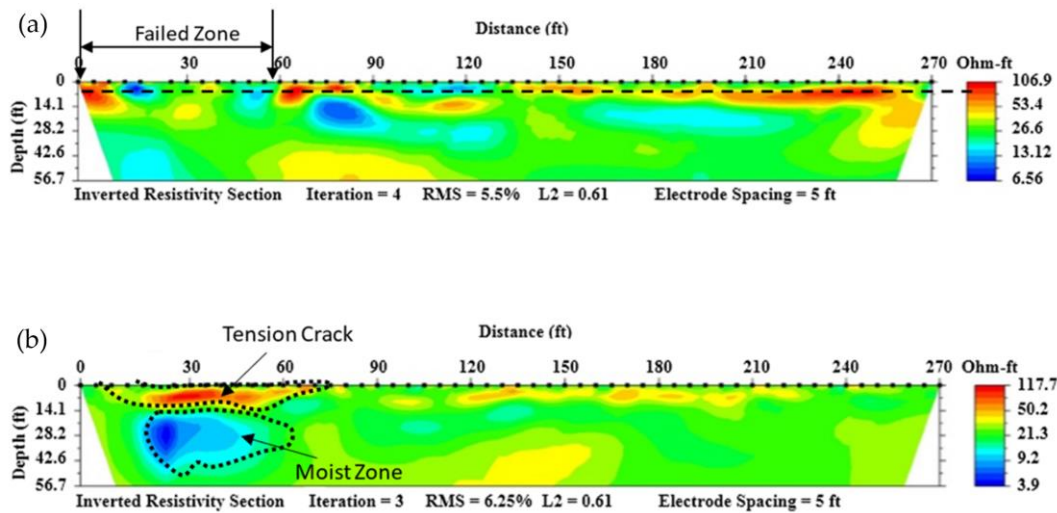


Figure 14. (a) Test results of the resistivity line RL-1 (at crest); (b) test results of the resistivity line RL-2 (at the middle of the slope).

The RL-2 was conducted over the tension crack at the middle of the slope (Figure 13b). A high-resistivity zone was observed immediately below the tension crack zone in the resistivity profile RL-2 (Figure 14b) where the depth of the high-resistivity zone was 3.65 m (12 feet). It should be noted that soil cracks create pathways for air to penetrate the soil, displacing moisture. Air has much higher resistivity compared to water or soil particles. This increase in air content within the cracks raises the overall resistivity of the soil. As a result, when electrical current passes through the soil and encounters these cracks, it encounters higher resistance due to the presence of air pockets. In addition, the soil dries out due to drying and shrinkage of soil. As soil dries out, its moisture content decreases.

Since water is a good conductor of electricity compared to soil particles, the reduction in moisture content leads to an increase in resistivity. Thus, soil cracks, by reducing moisture content locally, contribute to higher overall resistivity.

3.4. Case Study 4: ERT in Landfill ET Cover to Determine Moisture Variation

Water balance cover (or ET cover) has gained considerable attention over the last two decades as it offers a sustainable approach to the final capping of waste facilities [42]. The hydraulic performance of the ET cover system relies on the integrated soil–plant interaction. The field hydrologic performance of the water balance cover is significantly affected by soil hydraulic properties such as permeability and the soil water retention curve (SWRC). These hydraulic parameters significantly affect the drainage rate (percolation) to the waste mass below the cover [43–45]. The laboratory-experimented soil hydraulic behavior does not necessarily remain stable in the field throughout its service life. The post-construction natural processes such as insect and animal burrowing, freezing–thawing cycle, wetting–drying cycle, and root growth and death alter the textural orientation of the cover soil, thereby changing the hydraulic characteristics of the cover system. Therefore, the objective of performing resistivity tomography in the test section ET covers (lysimeter) was to investigate the seasonal pattern of moisture–suction variation in the lysimeter soil in a broader spectrum. The resistivity test was conducted every month. However, the frequency of field investigation was increased to once a week during summer (June–August), as moderate- to high-intensity rainfall coincided with high temperatures during that time. The results obtained through the resistivity tomography method yielded a clear identification of the covers’ moisture–suction undulation under fluctuating weather. Additionally, the field-investigated ERT data were discovered to be highly correlated with in situ unsaturated soil properties [46] and soil water storage [47].

3.4.1. Description

Large-scale test sections (Lysimeter) were built on an existing intermediate landfill cover with dimensions of 12 m × 12 m × 1.2 m at the investigation site: City of Denton landfill, Denton, Texas. At the bottom of the test section (subgrade), a geomembrane was placed, overlain by a geocomposite drainage layer. Then, the cover soil had 304.8 mm of surface layer underlain by 914 mm of compacted storage layer. Since the depth of the test sections was 1.2 m and the geomembrane layer was laid at the lysimeter subgrade, a total of 28 electrodes were considered for this study, with 152.4 mm spacing on a 4116 mm line, so that the resistivity profile could be obtained within 1220 mm (48 inches) depth. The field setup of RI testing is shown in Figure 15.

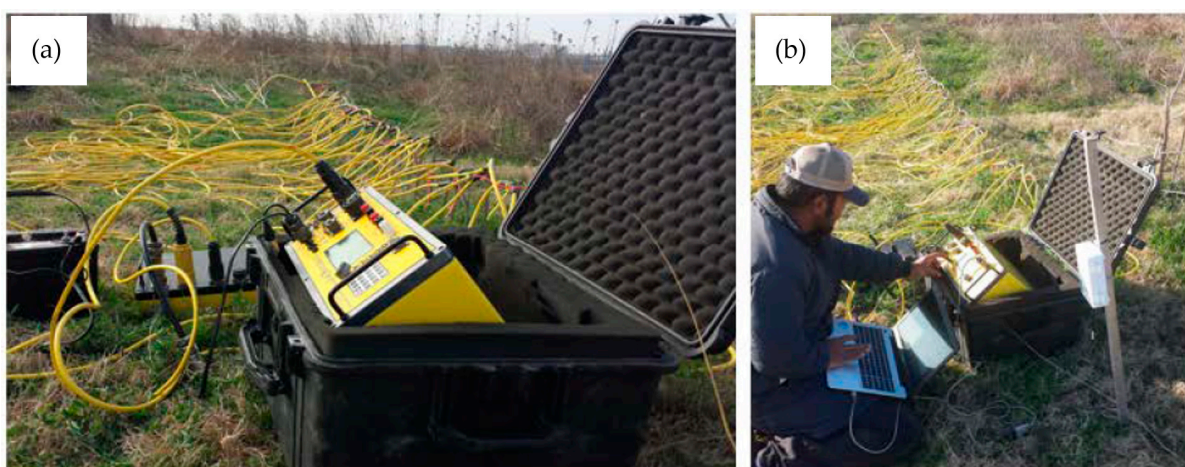


Figure 15. (a) Field setup with resistivity meter; (b) execution of ERT test.

3.4.2. Result

The ERT test was conducted at the site for three years from January 2015 to December 2017. For convenience, only a few field investigation plots of one lysimeter are shown in the manuscript. Resistivity profiles after a few extreme weather conditions in the summer of 2016 are presented in Figure 16, since several high-intensity rainfalls, along with high atmospheric temperatures, were recorded during that time. A clear distinction can be observed in the resistivity profiles. In Figure 16a,b, the bottom of the cover displays a low-resistivity zone (blue contour) indicating the existence of high moisture (saturated or near saturation) and, thereby, lower suction. The blue contour at the bottom of the cover signifies the potential drainage (percolation) from the cover. This notion of percolation perceived from the resistivity profiles was verified with the actual field percolation collection system. It was observed that significant percolation occurred during that time. Though the percolation data were not quantified from the resistivity data, the qualitative assessment of the resistivity profiles immediately provided obviousness of percolation. It should be highlighted that the top 304.8 mm to 457.2 mm depth of the cover exhibited a moderate- to high-resistivity zone, implying moisture loss to the environment through the evapotranspiration process.

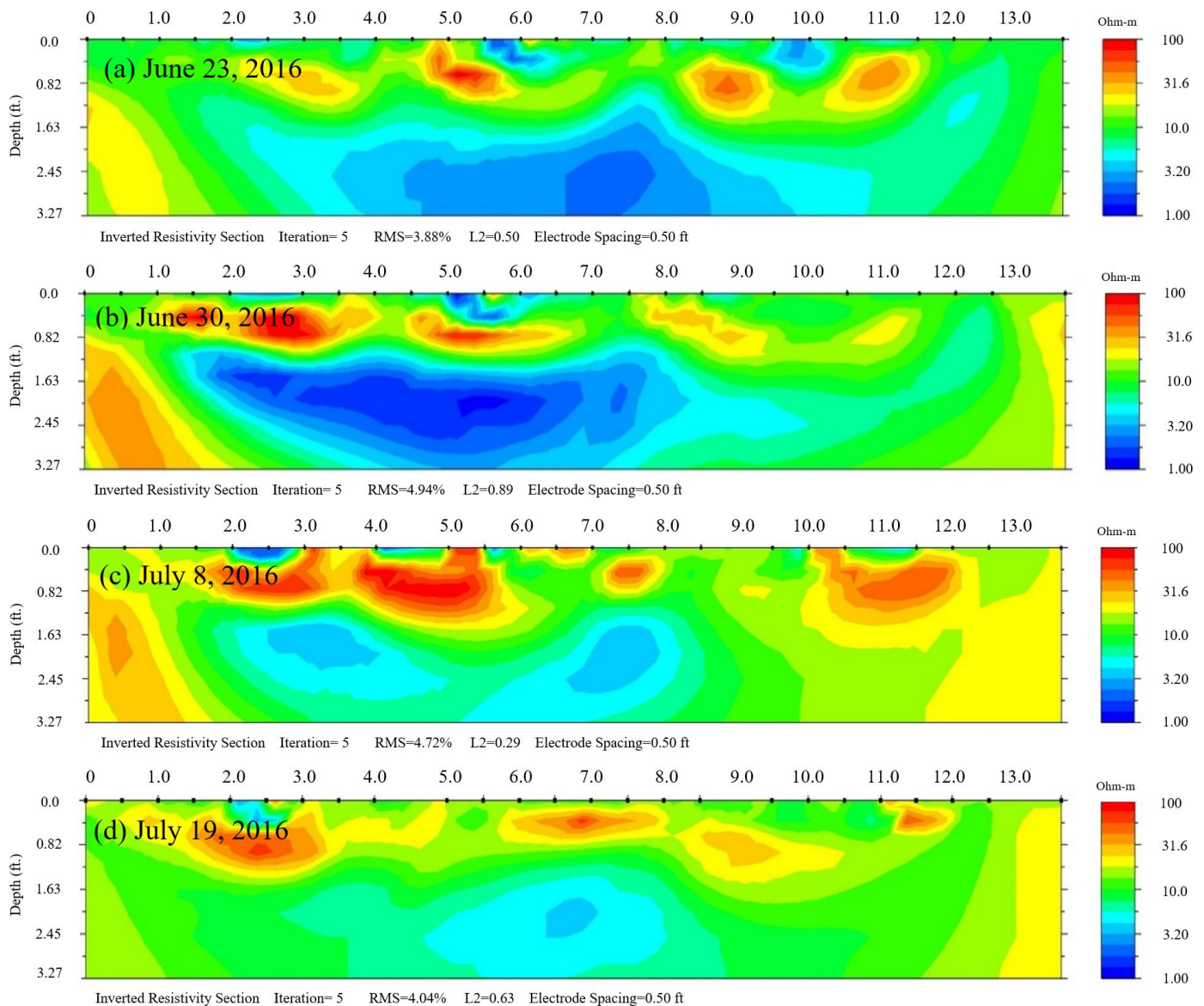


Figure 16. Resistivity tomography results of lysimeter-2.

In Figure 16c,d, the low-resistivity zone (blue contour) disappeared from the bottom of the cover, which illustrates the reduction in the degree of saturation of the cover soil. It was also noticed that the top 304.8 mm to 457.2 mm of the cover reached a higher-resistivity zone (increased suction and lower moisture content). Though several rainfall events were recorded during that time, the prevailing high temperature accelerated the evapotranspiration, consequently drying the top of the cover. One interesting fact was discovered in this study. The high-resistivity zone was predominantly observed in the top 304.8 mm to 457.2 mm. The different vegetation used in lysimeters in this study had root growth up to 508 mm [46]. Therefore, the moisture loss or evapotranspiration mainly occurred from the top (up to approximately 50 mm) of the cover soil. This study revealed that the ERT method is very effective in evaluating the seasonal moisture variation of ET cover soil. Furthermore, the qualitative assessment of the resistivity profile provided a strong indication of the crucial water balance component of this cover system.

4. Discussion

In the paper, four case studies were highlighted, where the electrical resistivity tomography (ERT) method was used in geotechnical (slope, pavement) and geoenvironmental (leachate recirculation, ET cover) applications. The findings from the field applications are quite interesting. ERT can be successfully used during the forensic investigation of slope failure, seasonal moisture variation of pavement, leachate recirculation frequency determination in landfills, and hydraulic performance evaluation of ET cover systems. The summary that can be drawn from these four case studies is provided below:

- For leachate recirculation in landfills for ELR operation, it was perceived that moisture in the waste mass reaches the equilibrium condition after approximately 14 days. The ERT method adequately captured the moisture distribution which assisted in reaching this conclusion.
- The perched water zone was satisfactorily located using ERT during a slope failure investigation along a state highway. The failed portion of the slope was repaired accordingly after the extent of failure depth and moisture-prone zone were detected based on the ERT investigation.
- Seasonal moisture variation in the pavement was successfully captured using the ERT method. From two years of field investigation, May–October was found to be the dry period, whereas November–April was recorded as the wet season.
- Moisture–suction relationship of the ET cover soil was recorded via ERT testing. The top few inches of the cover soil (root zone) exhibited a significant change in resistivity values in different seasons of the year, indicating the efficiency of ERT in evaluating the seasonal moisture variation of ET cover soil. These findings were later correlated with the percolation of the ET cover.

Author Contributions: Conceptualization, A.A. and M.J.B.A.; methodology, A.A.; software, A.A.; validation, A.A., M.J.B.A., and M.Z.A.; formal analysis, A.A. and M.J.B.A.; investigation, A.A. and M.J.B.A.; resources, A.A.; data curation, A.A.; writing—original draft preparation, A.A. and M.J.B.A.; writing—review and editing, A.A. and M.J.B.A.; visualization, M.Z.A.; supervision, M.Z.A.; project administration, M.Z.A. All authors have read and agreed to the published version of the manuscript.

Funding: The case studies presented here were funded by the Texas Department of Transportation and the City of Denton Landfill in Texas (2014–2017).

Data Availability Statement: No new data were created or analyzed in this study. Data sharing does not apply to this article.

Conflicts of Interest: The authors declare no conflicts of interest. The funders had no role in the design of the study; in the collection, analyses, or interpretation of data; in the writing of the manuscript, or in the decision to publish the results.

References

1. Tabbagh, A.; Dabas, M.; Hesse, A.; Panissod, C. Soil resistivity: A non-invasive tool to map soil structure horization. *Geoderma* **2000**, *97*, 393–404. [[CrossRef](#)]
2. Samouëlian, A.; Cousin, I.; Tabbagh, A.; Bruand, A.; Richard, G. Electrical Resistivity Survey in Soil Science: A Review. *Soil Tillage Res.* **2005**, *83*, 173–193. [[CrossRef](#)]
3. Aizebeokhai, A.P. 2D and 3D geoelectrical resistivity imaging: Theory and field design. *Sci. Res. Essays* **2010**, *5*, 3592–3605.
4. Jabrane, O.; Martínez-Pagán, P.; Martínez-Segura, M.A.; Alcalá, F.J.; El Azzab, D.; Váscquez-Maza, M.D.; Charroud, M. Integration of Electrical Resistivity Tomography and Seismic Refraction Tomography to Investigate Subsiding Sinkholes in Karst Areas. *Water* **2023**, *15*, 2192. [[CrossRef](#)]
5. Martínez-Pagán, P.; Gómez-Ortiz, D.; Martín-Crespo, T.; Manteca, J.; Rosique, M. The electrical resistivity tomography method in the detection of shallow mining cavities. A case study on the Victoria Cave, Cartagena (SE Spain). *Eng. Geol.* **2013**, *156*, 1–10. [[CrossRef](#)]
6. Ghorbani, A.; Revil, A.; Bonelli, S.; Barde-Cabusson, S.; Girolami, L.; Nicoleau, F.; Vaudelet, P. Occurrence of sand boils landside of a river dike during flooding: A geophysical perspective. *Eng. Geol.* **2024**, *329*, 107403. [[CrossRef](#)]
7. Franco, L.M.; La Terra, E.F.; Panetto, L.P.; Fontes, S.L. Integrated application of geophysical methods in Earth dam monitoring. *Bull. Eng. Geol. Environ.* **2024**, *83*, 62. [[CrossRef](#)]
8. Hinojosa, H.R.; Kirmizakis, P.; Soupios, P. Historic Underground Silver Mine Workings Detection Using 2D Electrical Resistivity Imaging (Durango, Mexico). *Minerals* **2022**, *12*, 491. [[CrossRef](#)]
9. Bharti, A.K.; Singh, K.K.K.; Ghosh, C.N.; Mishra, K. Detection of subsurface cavity due to old mine workings using electrical resistivity tomography: A case study. *J. Earth Syst. Sci.* **2022**, *131*, 39. [[CrossRef](#)]
10. Arjwech, R.; Ruansorn, T.; Schulmeister, M.; Everett, M.E.; Thitimakorn, T.; Pondthai, P.; Somchat, K. Protection of electricity transmission infrastructure from sinkhole hazard based on electrical resistivity tomography. *Eng. Geol.* **2021**, *293*, 106318. [[CrossRef](#)]
11. Suzuki, K.; Toda, S.; Kusunoki, K.; Fujimitsu, Y.; Mogi, T.; Jomori, A. Case studies of electrical and electromagnetic methods applied to mapping active faults beneath the thick quaternary. *Dev. Geotech. Eng.* **2000**, *84*, 29–45.
12. Beauvais, A.; Ritz, M.; Parisot, J.-C.; Bantsimba, C.; Dukhan, M. Combined ERT and GPR methods for investigating two-stepped lateritic weathering systems. *Geoderma* **2004**, *119*, 121–132. [[CrossRef](#)]
13. Maillot, G.M.; Rizzo, E.; Revil, A.; Vella, C. High resolution electrical resistivity tomography (ERT) in a transition zone environment: Application for detailed internal architecture and infilling processes study of a rhône river paleo-channel. *Mar. Geophys. Res.* **2005**, *26*, 317–328. [[CrossRef](#)]
14. Hauck, C. Frozen ground monitoring using DC resistivity tomography. *Geophys. Res. Lett.* **2002**, *29*, 12-1–12-4. [[CrossRef](#)]
15. Zhou, Q.Y.; Shimada, J.; Sato, A. Three-dimensional spatial and temporal monitoring of soil water content using electrical resistivity tomography. *Water Resour. Res.* **2001**, *37*, 273–285. [[CrossRef](#)]
16. Hossain, M.S.; Maganti, D.; Hossain, J. Assessment of geo-hazard potential and site investigations using Resistivity Imaging. *Int. J. Environ. Technol. Manag.* **2010**, *13*, 116–129. [[CrossRef](#)]
17. McCarter, W.J. The electrical resistivity characteristics of compacted clays. *Geotechnique* **1984**, *34*, 263–267. [[CrossRef](#)]
18. Abu-Hassanein, Z.S.; Benson, C.H.; Blotz, L.R. Electrical resistivity of compacted clays. *J. Geotech. Eng.* **1996**, *122*, 397–406. [[CrossRef](#)]
19. Ekwue, E.; Bartholomew, J. Electrical conductivity of some soils in Trinidad as affected by density, water and peat content. *Biosyst. Eng.* **2011**, *108*, 95–103. [[CrossRef](#)]
20. Kalinski, R.; Kelly, W. Estimating water content of soils from electrical resistivity. *Geotech. Test. J.* **1993**, *16*, 323–329. [[CrossRef](#)]
21. Gao, P.; Chung, S.; Kim, D.; Tanaka, H. Electric imaging and laboratory resistivity testing for geotechnical investigation of Pusan clay deposits. *J. Appl. Geophys.* **2003**, *52*, 157–175. [[CrossRef](#)]
22. Power, C.; Gerhard, J.I.; Karaoulis, M.; Tsourlos, P.; Giannopoulos, A. Evaluating four-dimensional time-lapse electrical resistivity tomography for monitoring DNAPL source zone remediation. *J. Contam. Hydrol.* **2014**, *162–163*, 27–46. [[CrossRef](#)]
23. Ali, M.A.H.; Sun, S.; Qian, W.; Dodo, B.A. Electrical resistivity imaging for detection of hydrogeological active zones in karst areas to identify the site of mining waste disposal. *Environ. Sci. Pollut. Res.* **2020**, *27*, 22486–22498. [[CrossRef](#)] [[PubMed](#)]
24. Ahmed, A.; Hossain, M.S.; Khan, M.S.; Greenwood, K.; Shishani, A. Moisture Variation in Expansive Subgrade through Field Instrumentation and Geophysical Testing. In Proceedings of the International Congress and Exhibition “Sustainable Civil Infrastructures: Innovative Infrastructure Geotechnology”, Sharm El Sheikh, Egypt, 15–19 July 2017; Springer: Cham, Switzerland, 2017; pp. 45–58.
25. Alam, M.Z.; Hossain, M.S.; Samir, S. Performance Evaluation of a Bioreactor Landfill Operation. In Proceedings of the Geotechnical Frontiers 2017, Orlando, FL, USA, 12–15 March 2017.
26. Ozcep, F.; Tezel, O.; Asci, M. Correlation between electrical resistivity and soil-water content: Istanbul and Golcuk. *Int. J. Phys. Sci.* **2009**, *4*, 362–365.
27. Hossain, M.S.; Khan, M.S.; Hossain, J.; Kibria, G.; Taufiq, T. Evaluation of unknown foundation depth using different ndt methods. *J. Perform. Constr. Facil.* **2013**, *27*, 209–214. [[CrossRef](#)]
28. U.S. Environmental Protection Agency (EPA). *Fact Sheet on Evapotranspiration Cover Systems for Waste Containment*; Office of Solid Waste and Emergency Response: Washington, DC, USA, 2011.

29. Binley, A. Tools and techniques: DC electrical methods. In *Treatise on Geophysics*, 2nd ed.; Schubert, G., Ed.; Elsevier: Amsterdam, The Netherlands, 2015; Volume 11, pp. 233–259.
30. Lerner, L.S. *Physics for Scientists and Engineers*; Jones & Bartlett Learning: Burlington, MA, USA, 1996; Volume 1.
31. Millikan, R.A.; Bishop, E.S. *Elements of Electricity: A Practical Discussion of the Fundamental Laws and Phenomena of Electricity and Their Practical Applications in the Business and Industrial World*; American Technical Society: Orland Park, IL, USA, 1917.
32. Manzur, S. Hydraulic Performance Evaluation of Different Recirculation Systems for ELR/Bioreactor Landfills. Ph.D. Thesis, The University of Texas at Arlington, Arlington, TX, USA, 2013.
33. Advanced Geosciences, Inc. *Instruction Manual for Earth Imager 2D Version 1.7.4: Resistivity and IP Inversion Software*; Advanced Geosciences, Inc.: Austin, TX, USA, 2004.
34. Manzur, S.R.; Hossain, S.; Kemler, V.; Khan, M.S. Monitoring extent of moisture variations due to leachate recirculation in an ELR/bioreactor landfill using resistivity imaging. *Waste Manag.* **2016**, *55*, 38–48. [[CrossRef](#)] [[PubMed](#)]
35. Shihada, H.; Hossain, M.S.; Kemler, V.; Dugger, D. Estimating moisture content of landfilled municipal solid waste without drilling: Innovative approach. *J. Hazard. Toxic Radioact. Waste* **2013**, *17*, 317–330. [[CrossRef](#)]
36. Buettner, M.; Daily, W.; Ramirez, A. *Electronic (sic) Resistance Tomography Imaging of Spatial Moisture Distribution, Moisture Distribution, and Movement in Pavements (Electrical Resistance Tomography for Monitoring the Infiltration of Water into a Pavement Section)*; FHWA/CA/OR-98-05; California Department of Transportation: Sacramento, CA, USA, 1997.
37. Clarke, C.R. Monitoring Long-Term Subgrade Moisture Changes with Electrical Resistivity Tomography. In Proceedings of the Fourth International Conference on Unsaturated Soils, Carefree, AZ, USA, 2–6 April 2006; American Society of Civil Engineers: Carefree, AZ, USA, 2006; pp. 258–268.
38. Hossain, S.; Ahmed, A.; Khan, M.S.; Aramoon, A.; Thian, B. Expansive Subgrade Behavior on a State Highway in North Texas. In Proceedings of the Geotechnical and Structural Engineering Congress, Phoenix, AZ, USA, 14–17 February 2016; American Society of Civil Engineers: Phoenix, AZ, USA, 2016; pp. 1186–1197.
39. George, A.M.; Chakraborty, S.; Das, J.T.; Pedarla, A.; Puppala, A.J. Understanding shallow slope failures on expansive soil embankments in north texas using unsaturated soil property framework. In Proceedings of the Second Pan-American Conference on Unsaturated Soils, Dallas, TX, USA, 12–15 November 2017; pp. 206–216.
40. Ahmed, A.; Khan, S.; Hossain, S.; Sadigov, T.; Bhandari, P. Safety prediction model for reinforced highway slope using a machine learning method. *Transp. Res. Rec. J. Transp. Res. Board* **2020**, *2674*, 761–773. [[CrossRef](#)]
41. Khan, M.S.; Hossain, S.; Ahmed, A.; Faysal, M. Investigation of a shallow slope failure on expansive clay in Texas. *Eng. Geol.* **2017**, *219*, 118–129. [[CrossRef](#)]
42. Benson, C.H.; Albright, W.H.; Roesler, A.C.; Abichou, T. Evaluation of final cover performance: Field data from the alternative cover assessment program (ACAP). *Proc. Waste Manag.* **2002**, *2*, 1–15.
43. Khire, M.; Benson, C.; Bosscher, P. Water Balance Modeling of Earthen Landfill Covers. *J. Geotech. Geoenviron. Eng.* **1997**, *123*, 744–754. [[CrossRef](#)]
44. Ogorzalek, A.S.; Bohnhoff, G.L.; Shackelford, C.D.; Benson, C.H.; Apiwantragoon, P. Comparison of field data and water-balance predictions for a capillary barrier cover. *J. Geotech. Geoenvironmental Eng.* **2008**, *134*, 470–486. [[CrossRef](#)]
45. Bohnhoff, G.L.; Ogorzalek, A.S.; Benson, C.H.; Shackelford, C.D.; Apiwantragoon, P. Field Data and Water-Balance Predictions for a Monolithic Cover in a Semiarid Climate. *J. Geotech. Geoenvironmental Eng.* **2009**, *135*, 333–348. [[CrossRef](#)]
46. Alam, M.J.B.; Hossain, M.S.; Sarkar, L.; Rahman, N. Evaluation of Field Scale Unsaturated Soil Behavior of Landfill Cover through Geophysical Testing and Instrumentation. In Proceedings of the Geo-Congress 2019: Eighth International Conference on Case Histories in Geotechnical Engineering, Philadelphia, PA, USA, 24–27 March 2019; pp. 1–11.
47. Bin Alam, J.; Sarker, L.; Sapkota, A.; Ahmed, R.; Hossain, S. Evaluation of Soil Water Storage (SWS) of Evapotranspiration Cover through Geophysical Investigation. In Proceedings of the Geo-Congress 2020, Minneapolis, MN, USA, 25–28 February 2020; pp. 444–453.

Disclaimer/Publisher’s Note: The statements, opinions and data contained in all publications are solely those of the individual author(s) and contributor(s) and not of MDPI and/or the editor(s). MDPI and/or the editor(s) disclaim responsibility for any injury to people or property resulting from any ideas, methods, instructions or products referred to in the content.